

Nonequilibrium state and lattice instability in supersaturated aluminum silicon solid solutions

J. Chevrier

Centre de Recherche sur les Mécanismes de la Croissance Cristalline, Centre National de la Recherche Scientifique, Campus de Luminy, case 913, 13288 Marseille Cedex 9, France

J. B. Suck

Institut Laue Langevin, Boîte Postale 156, 38042 Grenoble Cedex 9, France

J. C. Lasjaunias

Centre de Recherches sur les Très Basses Températures, Centre National de la Recherche Scientifique, Boîte Postale 156X, 38042 Grenoble Cedex, France

M. Perroux and J. J. Capponi

Laboratoire de Cristallographie, Centre National de la Recherche Scientifique, Boîte Postale 156X, 38042 Grenoble Cedex, France

(Received 17 May 1993)

Nonequilibrium AlSi solid solutions have been prepared by means of thermal annealing ($T \sim 1000$ K) at high pressure ($P \sim 4$ GPa). This synthesis is possible due to the metallic character of silicon under high pressure which greatly enhances the solubility of silicon in aluminum. The study of these supersaturated AlSi solid solutions has enabled us to investigate the chemical destabilization of a crystalline lattice. We experimentally show by means of inelastic neutron scattering and low-temperature specific heat that, as the silicon concentration in the aluminum lattice is enhanced, transverse acoustic phonon modes are becoming softer. This corresponds to a dramatic decrease of the shear modulus. Using differential scanning calorimetry, the positive heat of silicon dissolution in aluminum is measured under normal pressure: $\Delta H = 38$ kJ/mole. We interpret it as being mainly due to the energy difference between a metallic bonding of silicon in aluminum compared to its usual covalent bonding after demixing. This large heat of dissolution appears as the major reason for the observed lattice instability. Comparison of our experimental results with corresponding effects observed in usual amorphous metals suggests that further increase of the silicon concentration would induce a structural transformation of this crystal if the silicon segregation could be prevented.

INTRODUCTION

The existence of amorphous materials in a nonequilibrium state, obtained directly from the crystal without melting, raises the question of the increasing instability of a crystal driven further and further away from its equilibrium state at a temperature much lower than the temperature of the melting point and ultimately of its possible amorphization due to a mechanical instability.¹ The topological instability of chemically disordered crystalline solid solutions far from equilibrium has been introduced to describe this situation.^{2,3} Mechanisms for collective atomic displacements have been proposed in order to describe the transformation of a crystalline but chemically disordered solution into an amorphous state.³ In this analysis, the local shear stress field, mainly due to large differences in atomic size of alloy constituents, has been identified as a root of the occurrence of structural disordering.² Indeed thresholds of solute concentrations large enough to induce an amorphous state instead of a crystalline extended solid solution during rapid solidification have been estimated in a quite good agreement with experimental results. These arguments associate the amorphization by disordering of the crystalline state with (i) a nonequilibrium crystalline state, (ii) a change of mac-

roscopic elastic properties and (iii) a stress field varying on a very short scale. Besides the atomic disorder, these are definitely major experimental features of the amorphous state. This is experimentally shown by (i) the large irreversible heat released at crystallization compared to the latent heat of melting,⁴ (ii) the reduced shear modulus of the amorphous state compared to the crystalline state^{5,6} and (iii) the anomalous thermal properties attributed to the low-energy excitations⁶ (which are usually described by the phenomenological model of two level systems). Experimental investigations of the relative stability of an amorphous phase compared to the corresponding crystalline solid solution can be found in recent thermodynamical studies.⁷ The change of elastic properties and the appearance of a lattice instability in nonequilibrium solid solutions have been described in Refs. 8 and 1. Also the change of the shear resistance of thin films during disordering by irradiation is experimentally shown in Ref. 9 (however this is a different problem compared to the lattice instability of a crystal with almost no disorder on the atomic positions). These analysis and experiments suggest that a description of both, the local atomic displacements and the softening of the phonon modes during amorphization, is presumably a required information to understand the transformation of unstable crystals to

amorphous materials. As a first step toward this goal, one can investigate the change of the dynamical properties of a crystal as it is driven further and further away from its equilibrium state.

In this paper, we show that in the case of silicon dissolved in fcc aluminum, it is possible to prepare highly supersaturated solid solutions and to relate the origin of the nonequilibrium state to the chemical interaction between the metallic aluminum and the usually covalent silicon. There is a very important difference in the mechanism of destabilization compared to the aforementioned size effect. We shall see that in the fcc aluminum matrix, the silicon atomic size is very close to that of aluminum¹⁰ and that the large positive heat of mixing is in fact due to the electronic transition of silicon from a covalent bonding to a metallic bonding. This is very close to the effect invoked in Ref. 11 to analyze the formation of amorphous AuSi by rapid quenching from the melt. For AlSi solid solutions, these remarks will be experimentally justified by differential scanning calorimetry measurements. The importance of the silicon metallic state will also directly appear in the preparation of samples by quenching under high pressure. At atmospheric pressure, silicon has a very limited solubility in the fcc lattice of aluminum. Under very high pressure, silicon becomes metallic and completely transforms the metallurgy of AlSi alloys with the appearance of a large solubility of silicon in aluminum at least at high temperature.^{12,13}

The lowest silicon concentration we shall consider here is 4 at. %. This already corresponds to a concentrated solid solution in which the silicon atoms cannot be considered as isolated randomly distributed impurities. Furthermore all the experimental results we present in this paper give averaged properties of these materials. Neither the behavior of the silicon atoms nor the aluminum lattice around impurities are locally investigated by our experiments. However the AlSi solid solutions are supersaturated and therefore in a nonequilibrium state, even at very low silicon concentration [the solubility is respectively 1.6 at. % and 0.05 at. % of silicon at the solidus temperature, $T=577^{\circ}\text{C}$, and at $T=300^{\circ}\text{C}$ (Ref. 12) and even less than that at room temperature]. This raises the question of the local dynamical properties around one impurity and of its experimental observation. A discussion of this point cannot be inferred from our measurements but this question is in fact the subject of recent experiments on local dynamical properties in diluted solid solutions.^{14,15} They indicate a large softening of the host matrix around isolated impurities. In PbSn solid solution, the change of the dynamical properties of the Pb matrix around a Sn impurity is so large that authors describe it as a local melting. The estimated size of the soft zone is about 8 Å. Such a result leads us to consider the elastic interaction between randomly distributed impurities as the concentration is increased. It may be of interest to experimentally investigate the cross over between a local change of dynamical properties and the average softening of the elastic properties.

In this article we present a detailed analysis of AlSi solid solutions for silicon concentration between 4 and 10%. This range of concentration appears to lie in be-

tween the two aforementioned regimes. Experiments have been performed in order to characterize *simultaneously* the nonequilibrium state of these supersaturated solid solutions and their dynamical properties. The nonequilibrium state has been studied by differential scanning calorimetry (DSC) to measure the enthalpy release during thermal annealing. Inelastic neutron has been used together with the measurement of the low-temperature specific heat to characterize the variation of the dynamical properties together with electronic and superconducting properties.

EXPERIMENT

Sample preparation and characterization: Using commercial pure aluminum (5N) and silicon of electronic quality, we have prepared master ingots with atomic concentrations $\text{Al}_{1-x}\text{Si}_x$ ($x=0.04; 0.06; 0.08$ and 0.1). They were polycrystalline mixture of aluminum and silicon grains both identified in neutron and x-ray powder diffraction pattern. To dissolve the silicon in the fcc aluminum matrix, cut pieces of the master ingots have been put under high pressure $P\sim 4$ GPa at a temperature of about 1000 K during one hour. After the complete dissolution of silicon in the fcc Al matrix, the samples were quenched down under pressure to room temperature in about 10 s. The quenching rate is provided by the thermal contact of the sample with the belt system kept at room temperature. After quenching, the pressure was released. The samples were kept at the temperature of liquid nitrogen under atmospheric pressure. They were small cylinders roughly 9 mm in diameter and 6 mm height. They were characterized by means of standard x-ray powder diffraction and by neutron powder diffraction on the instruments *D1B* and *D1A* at Institut Laue Langevin. Compared to what is observed for the demixed master ingots, i.e., for AlSi alloys at equilibrium under atmospheric pressure at room temperature, the silicon diffraction peaks have disappeared in the quenched state due to the dissolution of the silicon atoms into the aluminum matrix. The same effect was seen in x-ray measurements. Thus for all the concentrations investigated, our samples appeared as homogeneous fcc AlSi solid solutions with no detectable silicon clusters. The final sets of samples (about 17 cm³ or 45 g) used for neutron inelastic scattering experiment were made of cylinders, all prepared under identical experimental conditions. In each case, the aluminum reference sample had the same geometry and same mass in order to have the best possible comparison. The same samples were used for differential scanning calorimetry experiments and measurements of the low-temperature specific heat.

DSC experiments: Small pieces of the samples (~ 10 mg) used for the neutron experiments were cut. While cutting the alloy, great care has been taken to avoid heating of the sample above 50°C. Using a Mettler Calorimeter, the enthalpy release has been measured at different heating rates (5, 10, 20, 40 K/min) for each concentrations. Even at the lowest silicon concentration, the signal was quite large giving a well-defined peak. This enabled us to determine accurately the enthalpy release and even

the change in the DSC peak shape as the silicon concentration is changed.

Inelastic neutron scattering experiments: The inelastic neutron scattering experiments were performed at the High Flux Reactor of the Institut Laue Langevin. For the AlSi6% alloy, we have used the thermal neutron time of flight spectrometer IN4 with an energy of the incident neutrons $E_0 = 68$ meV (resolution: $\Delta E_0/E_0 = 4\%$) using scattering angles between 5 and 100° . Thus a complete sampling of the phonons of these coherent scatterers was guaranteed. Exactly the same corrections have been used for both the $\text{Al}_{0.94}\text{Si}_{0.06}$ sample and the aluminum reference. The results for this concentration have been published in Ref. 8. For concentrations AlSi4% and AlSi8%, we have used the cold neutron time of flight spectrometer IN6. The samples were investigated at 100 and 296 K with $E_0 = 4.7$ meV and scattering angles between 11 and 113° were used. Thus frequencies were sampled in a smaller region of reciprocal space than on IN4 and the shape of the measured neutron energy gain spectra is considerably influenced by the unusually steeply increasing resolution function of the time focussing spectrometer especially at high energy (which causes the strong broadening of the peak of longitudinal phonons around 36 meV in Fig. 3), even though at low energies the resolution is about a factor of 40 better than that of IN4 ($\Delta E_0 \sim 125 \mu\text{eV}$).

Besides the two AlSi solid solutions, pure aluminium with the same sample shape (cylinder made of 44 small cylinders as described above), the cylindrical thin walled Al sample container, a vanadium cylinder of the same dimensions as the sample holder for reasons of calibration, and the empty cryostat were measured also. All sample runs were performed with high statistical accuracy. During the sample changes, the AlSi solutions, usually kept under liquid nitrogen, had to be warmed to room temperature to avoid condensation of moisture on the sample before insertion into the cryostat. The inelastic spectrum obtained in neutron energy gain on IN6 could be separated from the region of the elastic peak at 1 meV. The remaining low-energy part of the phonon density of states was then completed using a Debye approximation [$G(h\omega) = b(h\omega)^2$] where b was fitted in order to smoothly join the Debye spectrum and the measured distribution. In these binary alloys with two different coherent neutron scatterers, the generalized phonon density of states (GPDOS) was determined from the weighted sum of all time of flight spectra. The procedure used to analyze the measured spectrum can be found in Ref. 15

Low-temperature specific heat: The specific heat has been measured between 0.12 and 7 K using a transient heat pulse technique over a time span between 1 and 10^2 s in a dilution cryostat.⁶ The mass of samples was usually between 1 and 2 g. In measurements of samples with very different masses, a difference of about 1% has been found. This shows the reproducibility of these measurements. The total sample holder calibrated in an independent experiment has been subtracted at each temperature. At the lowest temperature around 100 mK, the sample holder contribution was 0.5 erg/K compared to a total specific heat of about 1-2 erg/K. This is the worse case:

at higher temperature, the contribution of the sample is much larger than the specific heat of the sample holder. The general uncertainty on the measurement is of the order of a few percent.

RESULTS

DSC experiments: Figure 1 presents characteristic DSC scans obtained with AlSi alloys of different concentrations. The major results in these measurements is a large enthalpy release for all the silicon concentrations investigated, causing a peak in the dynamic DSC scan roughly centered at a temperature of $T = 200^\circ\text{C}$. The integrated peak intensities show that this enthalpy release is in the range 1-5 kJ/mole. An x-ray diffraction measurement before and after annealing clearly demonstrates, by the appearance of silicon diffraction peaks after annealing, that this enthalpy release is mainly due to the silicon precipitation out of the aluminum matrix into covalent silicon clusters. Also an analysis of the maximum temperature in each spectrum versus the heating rate indicates that the DSC peak is due to an activated process with an activation energy of about 1.3 eV. This is very close to the characteristic activation energy for silicon diffusion in aluminum. Therefore we conclude that the exothermal effect is associated with the decomposition of the nonequilibrium aluminum silicon solid solution. Another remarkable feature is the shift towards lower temperatures of the whole peak as the silicon concentration is increased. This is a direct experimental evidence of the enhanced instability of this solid solution as the silicon concentration is increased. For the different silicon concentrations, one can also measure the total enthalpy released during the exothermal effect. This result is shown in Fig. 2. The error bars present the dispersion for different measurements on several samples of the same composition and for different heating rates. The variation of ΔH with the silicon concentration is linear in our range of measurement. The slope is 38 kJ/mole of silicon. This can be considered as the enthalpy of dissolution of silicon in solid aluminum. As the aluminum silicon liquid solution is almost ideal,¹² this highly positive

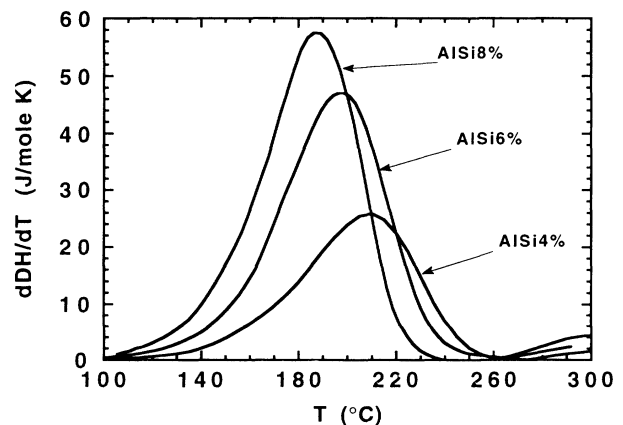


FIG. 1. DSC curves measured at $dT/dt = 10$ K/min for three different compositions of supersaturated aluminum silicon solid solution: AlSi4%, AlSi6%, and AlSi8%.

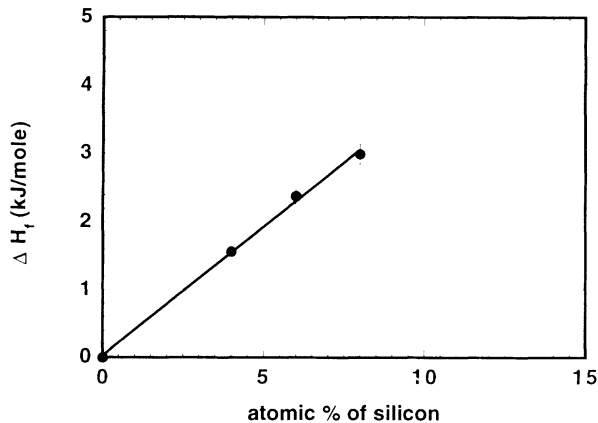


FIG. 2. Enthalpy variation due to complete segregation during annealing of aluminum silicon solid solution (integral of DSC spectra; see Fig. 1) vs the silicon concentration.

enthalpy of mixing is very much consistent with the shape of the simple eutectic phase diagram of the Al-Si system. A clear illustration of this, is presented in Ref. 17 using calculation of a phase diagram through the elementary quasicheical model with $\Delta H=0$ in the liquid state and $\Delta H=30$ kJ/mole in the solid state. However this consistency of our measurement of ΔH with the shape of the measured bulk phase diagram does not explain what is the origin of this large enthalpy of mixing in the solid state. The major contribution to the measured enthalpy of mixing can be deduced from several known experimental results.

During the decomposition of the solid solution, the silicon atoms undergo a major electronic change. They come from a metallic matrix of aluminum atoms to covalent clusters. A dramatic effect of this change is seen in the atomic volume of silicon. The atomic volume in pure fcc aluminum matrix is 16.6 \AA^3 whereas it is 20 \AA^3 in pure covalent silicon. The relevant volume to describe the state of silicon dissolved in aluminum is then certainly not the atomic volume in covalent silicon clusters but much more the atomic volume measured in the metallic silicon phases stabilized by high pressure. In the silicon β -Sn metallic phase, the first which is obtained when the hydrostatic pressure is increased, the atomic volume is 15.5 \AA^3 much closer to that of aluminum (16.6 \AA^3). This observation suggests that in order to estimate ΔH , one has to consider the energy change induced during the metal-semiconductor transition of silicon. Also it justifies the huge difference between the metallurgy of aluminum silicon alloys at normal pressure and under very high pressure. Under normal pressure, one has to deal with covalently bonded clusters embedded in a metallic matrix. For elements characterized by s and p electronic states, the major consequence of this is a phase diagram with very limited solid solutions. Under high pressure, the silicon is metallic. The electronic configuration of silicon is qualitatively close to the one of aluminum and basically described by the nearly free electron theory. With comparable atomic volumes, the large solubility of silicon in aluminum¹² is not very surprising. Such a large solubility is also what is seen in the metallic liquid state of the

aluminum silicon alloys which presents a small negative enthalpy of mixing. The influence of the silicon electronic transition is found in different situations. The first and obvious one is the melting of silicon with a latent heat of melting $L_f=49$ kJ/mole. This extremely large value does in fact account for the electronic transition at the melting point. A rough estimate of the contribution of the lattice disordering to the latent heat of melting is about 10 kJ/mole (The crystallization energy of amorphous silicon provides an experimental figure for this term.¹⁸ It is 11.5 kJ/mole). This gives an electronic contribution of about 39 kJ/mole. A second experimental indication for the value of ΔH is the study of the enthalpies of formation of different alloys like M -Al and M -Si ($M = \text{Fe, Co, Ni, } \dots$). Although its interpretation is quite complex, one has to take into account an extra contribution $\Delta H=37.7$ kJ/mole due to the metal-semiconductor transition of silicon¹⁹ in order to compare the measured and calculated enthalpies of formation for M -Si alloys. These different estimates of the characteristic energy associated with the electronic change of silicon are indeed very close to our experimental DSC results. We then conclude that the heat released during annealing of the quenched solid solution is, for its most important part, determined by the electronic transition of silicon from a metal to a semiconductor. This effect is the key point for the analysis of all subsequent experimental results presented in this paper. As previously mentioned, the source of the nonequilibrium state in these solid solutions is not the size difference between aluminium and the silicon atoms but the stabilization of the metallic state of silicon by the aluminum matrix.

Inelastic neutron scattering: In Fig. 3, phonon densities of states measured by inelastic neutron scattering for Al, AlSi4%, and AlSi8% are presented. The characteristic shape of the phonon density of states for an fcc structure is clearly identified. Below about 30 meV, the major contribution to the density of states is due to the transverse acoustic (TA) modes of vibrations whereas above 30 meV, the longitudinal acoustic (LA) modes are dominant. For both silicon concentrations AlSi4% and AlSi8%, the major result is the enhanced density of states at $E < 15$ meV and the reduced one for $15 \text{ meV} < E < 30 \text{ meV}$ compared

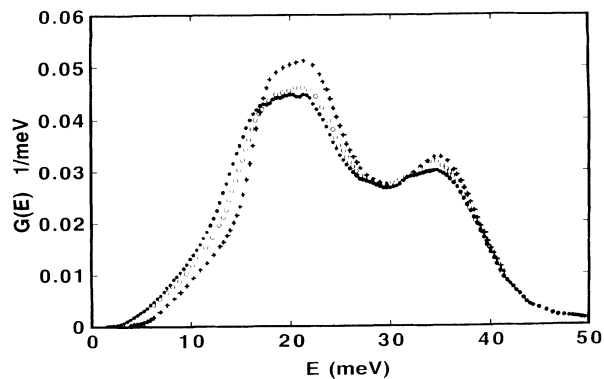


FIG. 3. Phonon frequency distribution of aluminum (+), AlSi4% (o), and AlSi8% (●) determined from cold neutron inelastic scattering experiments.

to aluminum. Thus this is a reproducible and strong feature that dissolution of silicon induces an enhancement of the phonon density of states at low frequency in the part of the curve where the TA modes are the most important. If one extrapolates these curves to the very low frequencies, these results imply a large decrease of the elastic shear modulus. Figure 3 also demonstrates that, as the number of silicon atoms substituting the aluminum atoms in the fcc lattice is increased, this softening of TA phonons becomes more important. This is an experimental evidence for the increased lattice instability due to the dissolution of silicon in the aluminum lattice. It is interesting to note that the magnitude measured here is very much comparable to a similar change of the dynamical properties measured for amorphous metals or metastable quasicrystalline phases in a nonequilibrium state^{16,20} relative to the corresponding crystallized samples. Hence looking at our data on AlSi solid solutions and other experimental studies on different materials in a nonequilibrium state, it is suggested that this phonon softening is linked with the nonequilibrium state of materials.

Low-temperature specific heat: In Figs. 4–6, the measurements of the specific heat for three different silicon concentrations, AlSi6%, AlSi8%, and AlSi10%, are presented. Above the superconducting transition temperature which is evidenced in these curves by a characteristic jump in the specific heat, the specific heat in this regime of temperature is well described by equation:

$$C_{p1}(T) = \gamma T + \beta T^3 \quad (1)$$

with no need for any correction term in this equation.

Figure 7 shows C_p/T versus T^2 plots for three different concentrations. The renormalized electronic density of states is determined from the contribution γT and the Debye temperature Θ_D from the phonon term βT^3 .

Figure 8 reports the variation of γ with silicon concentration. The most noticeable effect is a slight increase of

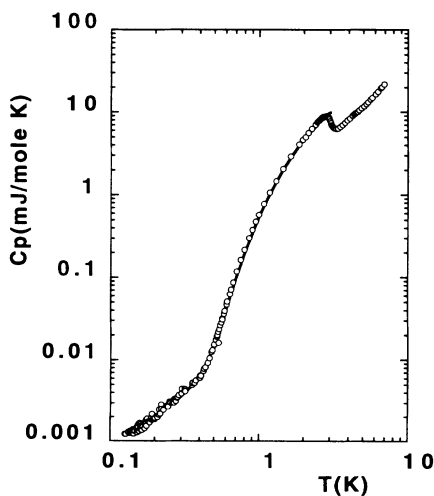


FIG. 4. Low-temperature specific heat of AlSi6% vs temperature. The solid line has been calculated using Eq. (4) with parameters $T_c = 3$ K, $\beta = 0.0343$ mJ/mole K⁴ ($\Theta_D = 384$ K), $\gamma = 1.47$ mJ/mole K², $\alpha = 0.01$ mJ/mole K².

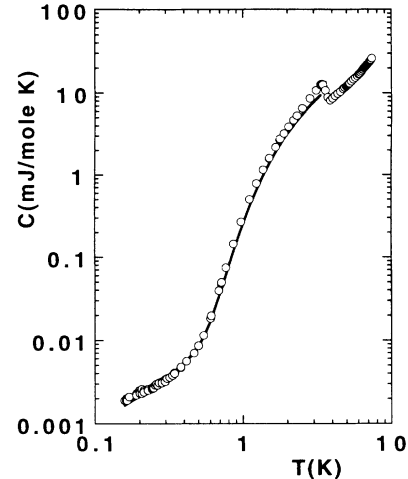


FIG. 5. Low-temperature specific heat of AlSi8% vs the temperature. The solid line has been calculated using Eq. (4) with parameters $T_c = 3.65$ K, $\beta^s = 0.020$ mJ/mole K⁴ (the measured value above T_c is $\beta^N = 0.039$ mJ/mole K⁴), $\gamma = 1.40$ mJ/mole K², $\alpha = 0.01$ mJ/mole K².

γ with silicon concentration. Such a small variation can be explained if one takes into account the metallic state of silicon in this solid solution. It is very consistent with the increase of the electron density due to the four valence electrons of silicon compared to three for aluminum. Figure 9 presents the variation of the Debye temperature with the silicon concentration. A large decrease of the Debye temperature is observed as the silicon concentration is increased. As the Debye temperature is mainly determined by the TA phonon modes in the low frequency limit, this is evidence for a large decrease of the shear modulus. Such a decrease of the Debye temperature is very much consistent with the enhanced phonon density of states measured by inelastic neutron scattering

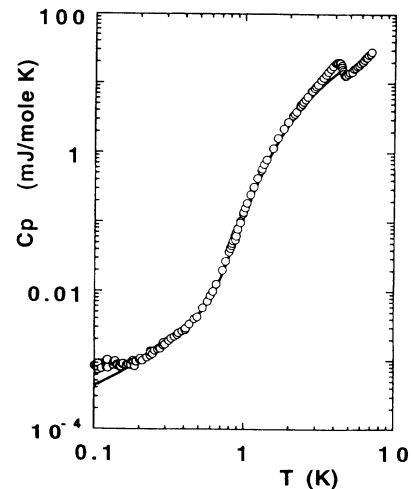


FIG. 6. Low-temperature specific heat of AlSi10% vs the temperature. The solid line has been calculated using Eq. (4) with parameters $T_c = 4.5$ K, $\beta^s = 0.020$ mJ/mole K⁴ (the measured value above T_c is $\beta^N = 0.052$ mJ/mole K⁴), $\gamma = 1.56$ mJ/mole K², $\alpha = 0.004$ mJ/mole K².

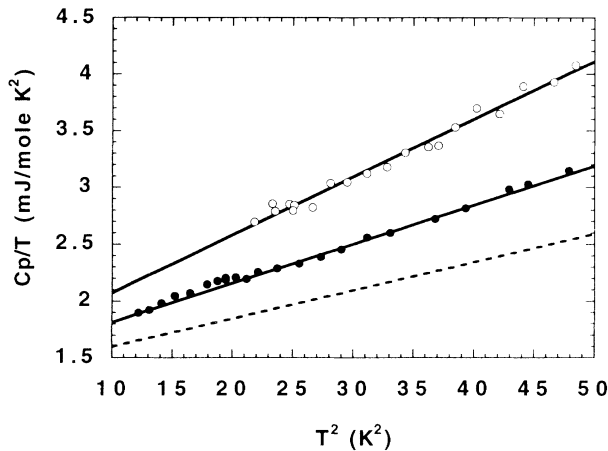


FIG. 7. C_p/T vs T^2 for different silicon concentrations investigated in the temperature range above T_c . For AlSi6% (●), the solid line is calculated with $\beta=0.0343$ mJ/mole K^4 ($\Theta_D=384$ K) and, $\gamma=1.47$ mJ/mole K^2 . For AlSi10% (○), the solid line is calculated with $\beta=0.052$ mJ/mole K^4 ($\Theta_D=334$ K) and, $\gamma=1.56$ mJ/mole K^2 . The line (---) is the calculated curve for aluminum with $\beta=0.0248$ mJ/mole K^4 ($\Theta_D=428$ K), $\gamma=1.35$ mJ/mole K^2 .

and can be seen as further evidence for the enhancement of the lattice instability as the silicon concentration is increased. A relative decrease of the shear modulus as large as 35% for the highest silicon concentration AlSi10% can be deduced from this change of Debye temperature following:

$$\Theta_D \propto \sqrt{\mu} \quad (2)$$

This is not the maximum change observed in nonequilibrium materials [as an example, the decrease of the shear modulus in CuZr amorphous metals is about 50% (Ref. 5)] but it is nearly as large. Experimentally the preparation of samples with even higher silicon concentrations is limited in our case by the rapid decomposition of the solid solution. However it would be of great interest to prepare samples with higher silicon concentrations in order to investigate the structural and dynamical behavior

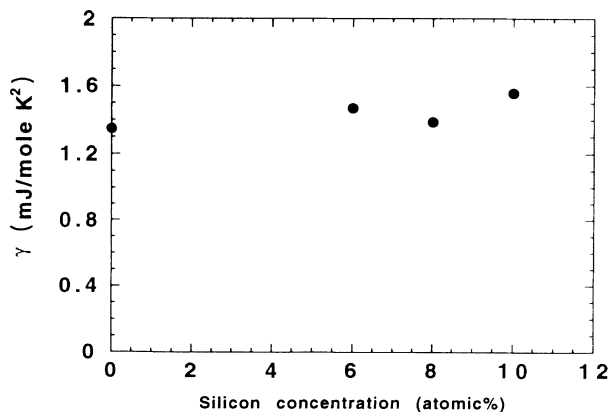


FIG. 8. Variation of the electronic contribution γ to the specific heat of AlSi solid solutions as the silicon concentration is varied.

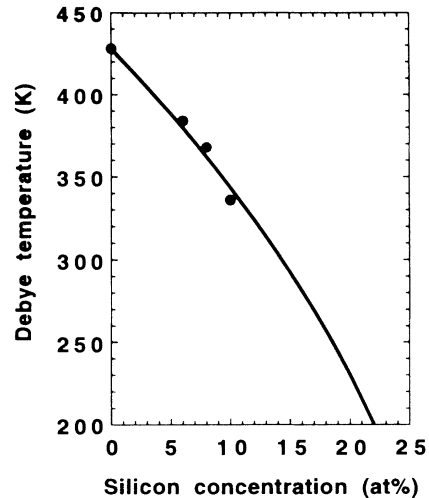


FIG. 9. Variation of the Debye temperature Θ_D of AlSi solid solutions as the silicon concentration is varied. The solid line is calculated using Eq. (4).

of samples as the shear modulus is further reduced.

An important effect observed in the specific heat measurements is the enhancement of the temperature of the superconducting transition. Starting with a T_c of 1.2 K for pure aluminum which is one of the materials best analyzed by the BCS theory, a T_c of 4.4 K is measured when 10% of silicon are dissolved in aluminum. The highest temperature of superconducting transition ever measured in these alloys is 11 K,¹³ an order of magnitude larger than the T_c of pure aluminum. Figure 10 presents the change of T_c in the high pressure quenched alloys as the silicon concentration is varied. Since only a minor part of the silicon may be segregated in these samples, this curve presents the intrinsic variation of T_c versus silicon concentration. The origin of the solid curve in Fig. 10 is

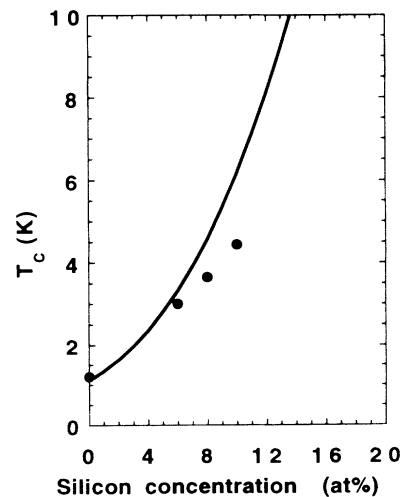


FIG. 10. Variation of the temperature of the superconducting transition T_c of AlSi solid solutions as the silicon concentration is varied. T_c is determined from the characteristic jump of the specific heat at the superconducting transition. The calculation of the solid line is presented in the discussion section of the text in Ref. 10.

presented in the following discussion.

At temperatures much lower than T_c , the specific heat of an fcc crystalline AlSi solid solution should follow:

$$C_{p2}(T) = 8.55\gamma T_c \exp(-1.44T_c/T) + \beta T^3. \quad (3)$$

Furthermore the phonon term βT^3 expected to be the one extrapolated from the high-temperature regime (i.e., $T > T_c$). The experimental results for different AlSi solid solutions show that this expression of the specific heat is not satisfactory. This calculated specific heat is smaller than the measured value. The shift is larger than the error bar. The plot of C_p/T versus T^2 in Fig. 11 at very low temperature for AlSi10% reveals a linear contribution. The same is correct for the two other silicon concentrations with contributions of the same order of magnitude. Thus specific heat measurements on AlSi solid solutions at different silicon concentrations, lead to an extra term at very low temperature. Below the temperature of the superconducting transition, the specific heat is well described by:

$$C_{p3}(T) = \alpha T + 8.55\gamma T_c \exp(-1.44T_c/T) + \beta T^3. \quad (4)$$

From our experiments, an averaged value of the coefficient of this linear term is $\alpha \sim 3 \cdot 10^{-7} \text{ J/g K}^2$ or $\alpha \sim 0.01 \text{ mJ/mole K}^2$. This is nearly an order of magnitude below the usual values measured in standard amorphous alloys ($\alpha \sim 0.05 \text{ mJ/mole K}^2$ for CuZr amorphous alloys). Using the expression of the specific heat calculated for a flat energy distribution of two level systems (TLS),²¹ one finds a "TLS density of states" of $n_0 = 0.32 \cdot 10^{41} \text{ J}^{-1} \text{ mole}^{-1}$. The purpose of this estimate is not to claim that the TLS model readily applies to the local dynamics of silicon impurities in the aluminum lattice. It only shows that the specific heat measurements are quite consistent with results of Ref. 22 where both the internal friction and the thermal conductivity have been

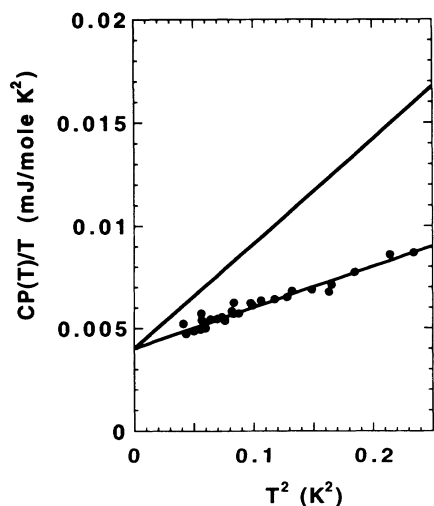


FIG. 11: C_p/T vs T^2 for the silicon concentration AlSi10% in the temperature range well below T_c . The fitting curve of the experimental points is $C_p/T \text{ (mJ/mole K}^2) = 0.004 + 0.02T^2$. The upper solid line uses the phonon contribution extrapolated from above T_c .

shown to be an order of magnitude different from amorphous metals. However whatever is the origin of the linear term observed in the specific heat, it appears very difficult to go any further towards a clear analysis of local dynamical properties around impurities on the basis of measurements of the specific heat or of the thermal conductivity in these particular alloys.

Another quite important measured effect for samples with composition AlSi10% is the change of the phonon term when measured at temperatures above or below T_c . The ratio of the two values of β is larger than 2 as it is seen in Fig. 11. This change is rather large and well characterized experimentally. It is also seen in the case of AlSi8% but with a smaller amplitude. No evidence for such a lattice hardening in the superconducting state is found for AlSi6%. In fact in different systems, this effect has already been observed. One can find several experimental reports of changes in the phonon contribution above and below T_c . This has either been found in crystalline materials²³ or in amorphous materials.^{24,6} Experimentally the condensation of electrons in the superconducting state is directly associated with this change.²³ Our measurements add another example to the set of systems exhibiting this property. To our knowledge, no satisfactory analysis of this complicated effect exists.

DISCUSSION

As shown in Refs. 10 and 25, it is possible to link the experimental values characteristic of the nonequilibrium state with dynamical properties through the equation:

$$\Theta_D(\text{Al}_{1-x}\text{Si}_x) = \Theta_D(\text{Al}) \sqrt{1-x[\Delta H/L_f(\text{Al})]}. \quad (5)$$

This equation is an extension of the approximate Lindeman criterion to materials in a nonequilibrium state.²⁶ The Lindeman criterion describes the lattice instability of a crystal as the temperature is raised. It is also²⁷ a relationship between the resistance against a macroscopic shear stress characterized by the shear modulus and the energy associated with the occurrence of rigidity and long-range order, i.e., with the latent heat of melting L_f . Compared to the latent heat of melting L_f which characterizes the rigidity of the fcc aluminum lattice, the enthalpy of dissolution $x\Delta H$ is associated with the change of the symmetry of silicon atoms when dissolved in this aluminum lattice. The difference $L_f - x\Delta H$ which enters Eq. (5) shows the decreasing resistance of the fcc lattice against shear stress due to the trapped silicon atoms. Using $L_f(\text{Al}) = 10.7 \text{ kJ/mole}$ and $\Theta_D(\text{Al}) = 428 \text{ K}$ with $\Delta H = 38 \text{ kJ/mole}$ of silicon, the change of the Debye temperature can be estimated with no adjustable parameter as the silicon concentration is varied. The result is shown as the solid line in Fig. 9. Likewise, it is possible to estimate the influence of the variation of the phonon spectra on the change of T_c in the framework of Mc Millan's analysis of superconductivity.²⁸ Such a procedure has been described in Ref. 8. The main input needed is the known characteristics of pure aluminum and it is not necessary to use any adjustable parameter. The result is the solid line in Fig. 10.

This rough analysis is by no means a complete descrip-

tion of the instability of AlSi solid solutions. Clearly more theoretical work is needed to quantitatively ascertain our interpretation.²⁹ The aim of our simple arguments is to state that the measured parameters presented in this article are physically connected and are different aspects of the same physical problem: the increasing instability of AlSi solid solutions as the silicon concentration is increased. It also definitely shows that the enhancement of the temperature of the superconducting transition which has received conflicting interpretations in the past, is mostly due to the softening of TA phonon modes. Using Eq. (5) for higher silicon concentrations, a Debye temperature of zero kelvin is obtained for a silicon concentration of 28 at. %. This would lead to a shear modulus continuously decreasing to zero. For a crystalline solid, a null shear modulus is clearly an unphysical situation and it is likely that, if silicon segregation can be avoided, a structural transformation would take place before such a high silicon concentration of 28% is reached. Nonetheless this illustrates how much more interesting it would be to investigate samples with higher silicon concentrations or to find another system in which the instability induced by the metallic state of silicon could be experimentally controlled until the lattice instability induces a structural transformation. Furthermore in this paper, we have been mainly concerned with macroscopic and average properties of these solid solutions. Our experimental results do not directly provide local information on the effect of the silicon dissolution on the aluminum lattice. Further studies on the increasing instability of supersaturated AlSi solid solutions would certainly require experimental methods more directly related to the local dynamic of silicon atoms.

CONCLUSION

An intrinsic consequence of the high supersaturation of AlSi solid solutions is their nonequilibrium state and the development of an important lattice instability. This lattice instability, resulting in a softening of TA phonons, appears to be the reason why the temperature of the superconducting transition is dramatically increased. The metallic state of silicon atoms in the fcc aluminum lattice is simultaneously the main cause of the nonequilibrium state and of the change of dynamical properties in these supersaturated crystalline solid solutions. The use of high pressure quenching to dissolve the silicon in aluminum directly emphasizes the change of electronic state from a covalent bonding to a metallic bonding of silicon atoms. Also due to the quality of samples prepared with this technique compared to the one of alloys rapidly quenched from the melt, quantitative results are obtained which could be compared to a model for the lattice instability in nonequilibrium solid solutions. Furthermore measurements which characterize the nonequilibrium state and the dynamical properties yield behaviors very close to what has been observed for other nonequilibrium materials like amorphous metals using the same experimental techniques. However this mainly concerns the macroscopic properties of the AlSi solid solutions. The only experimental result presented in this article which may be related to the local dynamic of silicon atoms in aluminum is the linear term in the specific heat. It is certainly not sufficient to characterize the existence of specific effects due to the disordered distribution of interacting impurities. Other experiments are needed to investigate this problem.

¹W. L. Johnson, *Prog. Mater. Sci.* **30**, 81 (1986).

²T. Egami and Y. Waseda, *J. Non-Cryst. Sol.* **64**, 113 (1984).

³J. M. Dubois, *J. Less Common Metals* **145**, 309 (1988).

⁴Z. Althounian, Tu Guo-hua, and J. O. Strom-Olsen, *J. Appl. Phys.* **53**, 4755 (1982).

⁵B. Golding, B. G. Bagley, and F. S. L. Hsu, *Phys. Rev. Lett.* **29**, 68 (1972); P. Garoche and P. Bigot, *Phys. Rev. B* **28**, 6886 (1983); J. E. Graebner and H. S. Chen, *Phys. Rev. Lett.* **58**, 1945 (1987).

⁶A. Ravex, J. C. Lasjaunias, and O. Bethoux, *J. Phys. F* **14**, 329 (1984).

⁷E. Ma and M. Atzmon, *Phys. Rev. Lett.* **67**, 1126 (1991).

⁸J. Chevrier, J. B. Suck, J. J. Capponi, and M. Perroux, *Phys. Rev. Lett.* **61**, 554 (1988).

⁹L. E. Rhen, P. R. Okamoto, J. Pearson, R. Bhadra, and M. Grimsditch, *Phys. Rev. Lett.* **59**, 2987 (1987).

¹⁰J. Chevrier, D. Pavuna, and F. Cyrot-Lackmann, *Phys. Rev. B* **36**, 9115 (1987).

¹¹H. S. Chen and D. Turnbull, *J. Appl. Phys.* **38**, 3646 (1967).

¹²J. L. Murray and A. J. McAlister, *Bull. Alloy Phase Diagrams* **5**, 74 (1984).

¹³V. F. Degtyareva, G. V. Chipenko, I. T. Belash, O. I. Barkalov, and G. Ponyatovskii, *Phys. Status Solidi A* **89**, K127 (1985).

¹⁴E. A. Stern and Ke Zhang, *Phys. Rev. Lett.* **60**, 1872 (1988).

¹⁵H. Shechter, E. A. Stern, Y. Yacoby, R. Brener, and Zhe Zhang, *Phys. Rev. Lett.* **63**, 1400 (1989).

¹⁶J.-B. Suck and H. Rudin, in *Glassy Metals*, edited by H. Beck and H. J. Güntherodt, Topics in Applied Physics Vol. 53 (Springer-Verlag, Berlin, 1983), p. 217; J.-B. Suck, H. Rudin, H. J. Güntherodt, H. Beck, J. Daubert, and W. Gläser, *J. Phys. C* **13**, L167 (1980).

¹⁷T. B. Massalski, *Met. Trans. A* **20A**, 1295 (1989).

¹⁸E. P. Donovan, F. Spaepen, D. Turnbull, J. M. Poate, and D. C. Jacobson, *Appl. Phys. Lett.* **42**, 698 (1983).

¹⁹A. Pasturel, thèse d'état Université de Grenoble, 1983.

²⁰J. B. Suck, H. Bretscher, H. Rudin, P. Grütter, and H. J. Güntherodt, *Phys. Rev. Lett.* **59**, 102 (1987).

²¹P. W. Anderson, B. I. Halperin, and C. M. Varma, *Philos. Mag.* **25**, 1 (1972); W. A. Phillips, *J. Low Temp. Phys.* **7**, 351 (1972).

²²J. E. van Cleve, J. Chevrier, and R. O. Pohl, in *Proceedings of the Conference Phonons 89, Heidelberg, 1989*, edited by S. Hunklinger, W. Ludwig, and G. Weiss (World Scientific, Singapore, 1990), Vol. 1, p. 579.

²³H. R. O'Neal and N. E. Phillips, *Phys. Rev.* **137**, 749 (1965).

²⁴C. Sürgers and H. von Löhneysen, *Z. Phys. B* **70**, 361 (1988).

²⁵J. Chevrier, J. C. Lasjaunias, F. Zougmore, and J. J. Capponi, *Europhys. Lett.* **8**, 173 (1989).

²⁶J. Chevrier, *Solid State Commun.* **65**, 1461 (1988).

²⁷J. K. Mackenzie and N. F. Mott, *Proc. Phys. Soc.* **63**, 411 (1950).

²⁸W. L. Mc Millan, *Phys. Rev.* **167**, 331 (1968).

²⁹A. Caro (unpublished).